
A

Presented to
the faculty of the School of Engineering and Applied Science
University of Virginia

in partial fulfillment
of the requirements for the degree

by

APPROVAL SHEET

This

is submitted in partial fulfillment of the requirements
for the degree of

Author:

Advisor:

Advisor:

Committee Member:

Committee Member:

Committee Member:

Committee Member:

Committee Member:

Committee Member:

Accepted for the School of Engineering and Applied Science:



Jennifer L. West, School of Engineering and Applied Science

Abstract

The development of hypersonic air breathing propulsion technology depends on wind tunnel testing and a large portion of this testing requires the use of optical measurement techniques. Unfortunately, a change in transmission of fused silica windows is possible in supersonic combustion facilities with long run times. This change can affect the utility of optical diagnostics as this transmission change occurs in the light wavelength band of 350 to 850 nm. This can prevent or disrupt Optical Emission Spectroscopy, Particle Image Velocimetry, Planar Laser Induced Fluorescence, and other techniques. In this study it was determined that the change in transmission was the result of devitrification of the window, which changed the silica from the amorphous form to cristobalite crystals. Cristobalite was detected through X-ray diffraction experiments and the amount was quantified for a used facility window. This is the first time window devitrification has been reported for a hypersonic ground testing facility. A sample of new fused silica was tested in a controlled oven environment to isolate high temperature as the main factor causing crystal formation. Identification of devitrification, and its cause, in a hypersonic ground testing facility, will aid in the application and interpretation of future optical diagnostics and presents facility operators with potential options for preventing it in the future.

Funding and Disclaimers

This work was supported by NASA's Space Technology Research Grants Program (NASA ULI Grant #80NSSC21M0069 P00001).

Acknowledgments

This thesis would not exist without the support of so many different people. First, I would like to thank my advisor Dr. Chris Goyne for supporting my work done in this thesis. I fell down quite the material science rabbit hole to write this, and this would not have been possible to complete without his support and keen insights throughout the process. Thank you as well to Dr. Chloe Dedic and Dr. Bob Rockwell who answered innumerable questions from me about all manner of things from the function of a white light source to answering key questions about facility operations. I am sure Dr. Rockwell is also relieved I am no longer operating the furnace at all hours of the day and no longer fears the lab burning down via furnace malfunction at three in the morning. I am also fortunate to have been supported by professionals outside the Department of Mechanical and Aerospace department, Dr. Diane Dickie in the Nanoscale Material Characterization Facility patiently trained me on the x-ray diffractometers and answered any questions I had.

A big thank you as well to all my friends and lab mates at the Aerospace Research Laboratory. This process would not have been nearly as fun without all of you giving your input, your support, and laughing with me when I melted a piece of glass to the floor. Being able to work with so many smart and driven people is a gift, and this fortune is not lost on me. A special thank you to Owen Petito for helping me with my optical setups, and Tyler Sussman for making me laugh when I needed it most.

There are so many other people in my life this thesis would not exist without either. My entire family: my parents, Linda and Ellis, who have always supported my scientific interests and endeavors from a young age, my Mom-Mom and Pop-Pop for their unyielding belief in my abilities, and my younger sister, Hannah, for her motivation. I owe all of you more than I can ever articulate for your love and support. I also have to say a big thank you to my housemates, Claire and David, who have learned more about glass than I'm sure they ever wanted to, and my dog Vera for reminding me to take breaks.

I also need to thank my partner Isa, who like everyone else mentioned probably learned more about glass than they ever wanted to. Thank you for being a voice of reason and my rock when I needed it the most. I only hope I can do the same for you, I love you.

Finally, I want to thank and acknowledge every scientist who has ever felt out of place in their studies. I stand on the shoulders of thousands upon thousands of scientists whose names and stories I will never know. I am grateful for their sacrifices and will strive to light the way for the next generation of researchers.

Table of Contents

<i>Abstract</i>	<i>i</i>
<i>Funding and Disclaimers</i>	<i>ii</i>
<i>Acknowledgments</i>	<i>ii</i>
<i>Table of Figures</i>	<i>iv</i>
1. Introduction	1
2. Experimental Methodology	5
2.1. Overall Experimental Approach	5
2.2. Measurements on Existing Facility Windows	5
2.2.1. Transmission and X-Ray Diffraction	5
2.3. Transmission of Samples in a Controlled Environment	8
2.3.1. Summary of Samples Used	8
2.3.2. Summary of Controlled Environment.....	9
3. Results	10
3.1. Existing Facility Windows	10
3.1.1. Transmission.....	10
3.1.2. X-Ray Diffraction	11
3.2. Controlled Environment Samples	12
3.2.1. Transmission.....	12
3.2.2. X-Ray Diffraction	13
3.3. Sapphire Samples	15
4. Discussion	15
5. Conclusion	17
<i>Appendix A – Sapphire Transmission Data</i>	18
<i>Bibliography</i>	19

Table of Figures

Figure 1a and 1b: Reported transmission for fused silica and sapphire glass from Esco Optics [9][10] 2

Figure 2: Three example windows, all three windows have been retired from use in testing. The window at the top of the photo is the window used in this study – the crack running across the width of the window occurred after all transmission and x-ray diffraction data was acquired. For transmission testing, location one is in red, location two is in blue..... 3

Figure 3: Experimental transmission setup (not to scale) Spectrometer was connected to a computer via USB..... 5

Figure 4a and 4b: Image of the Malvern-Panalytical Empyrean x-ray diffractometer in use (window circled in red) and simplified example of a x-ray diffraction setup for clarity..... 6

Figure 5: Reference XRD data used in Rietveld refinement 8

Figure 6: Temperature data from the furnace vs. stagnation temperature during a UVASCF test 9

Figure 7: Measured transmission of used window at two different versus new sample from Esco Optics. 10

Figure 8: X-ray diffraction data for used facility window 11

Figure 9: Change in transmission after heat cycle for controlled sample..... 13

Figure 10: X-ray diffraction data for sample before heat treatment 13

Figure 11: X-ray diffraction data for sample after heat treatment 14

Figure A: Sapphire sample transmission before and after heat treatment 18

1. Introduction

The term “hypersonic” is generally defined as any speed above Mach 5 and is associated with various phenomena such as shock waves that are thin and close to the body, the existence of an entropy layer with strong vorticity, viscous interaction between the boundary layer and inviscid flow, and ionization and dissociation of gas around the vehicle body, otherwise known as “high temperature effects” [1]. Given the nuance in the definition, it is critical to understand and characterize hypersonic combustion and flight testing with capable ground testing facilities.

There are multiple ways hypersonic travel can be achieved, including through rockets, but the future of sustained hypersonic travel is through the scramjet engine. Scramjets are functionally similar to their subsonic counterpart, the ramjet, but their combustion process is largely supersonic. In concept, scramjets capture air in an inlet and through geometrical compression, increase pressure, and reduce the Mach number. Fuel is then injected into the combustor section of the engine and combusted by the compressed air. An exhaust nozzle provides thrust. This method results in higher specific impulse, and thus more efficiency, than for the engine’s rocket counterpart. Notable successful flights as part of the X-43 and X-51 programs have occurred, for example [2], [3], [4].

Scramjet engines are still in development with a specific need for ground testing and characterization. The University of Virginia Supersonic Combustion Facility (UVASCF) is one such facility aimed at fulfilling this research need. The UVASCF is an electrically heated, vertically oriented, direct-connect combustion tunnel with unlimited runtime. In this facility there two large windows are located directly on either side of the typical flameholding section. The facility simulates Mach 5 enthalpies with a stagnation temperature of 1,200K (927°C), but higher temperatures are reached within flameholding regions. These regions are near to the primary windows discussed above and have been measured to reach temperatures ranging from 1,100K (827°C) to temperatures in excess of 2,000K (1727°C) [5].

The UVASCF is able to accommodate multiple optical diagnostics used by different research groups and with different requirements for wavelength transmission. This includes Planar Laser Induced Fluorescence (PLIF), commonly exciting OH, CH, CO, and OH and primarily relying on a wavelength of 283.8nm [6]. In addition, wavelengths used for Coherent Anti-Raman Scattering (CARS) depends on the type of CARS experiment being performed, but general key wavelengths include 400nm, 532nm, 674nm, and 800nm [7]. Further, Particle Image Velocimetry (PIV) can be applied to the facility. This technique is typically reliant light at as 527nm and 532nm for the use of Nd:YLF and Nd:YAG lasers, respectively. Finally, the UVASCF is capable of the application of Optical Emission Spectroscopy (OES). This method ideally uses the entire visible range of light, but specifically in some studies the ranges of 295nm-330nm, 412-440nm, and 495nm-520nm are used [8]. The windows in the UVASCF are composed of UV-fused silica sourced from Esco Optics; a material chosen specifically for its consistently high transmission from approximately 200nm-2000nm as seen in Figure 1a. Figure 1b is included as a reference for

another glass option, sapphire glass, which is known to be heat resistant but lacks the same transmission characteristics as UV-fused silica at lower wavelengths. These two materials serve as the primary window material of choice for many hypersonic ground test facilities.

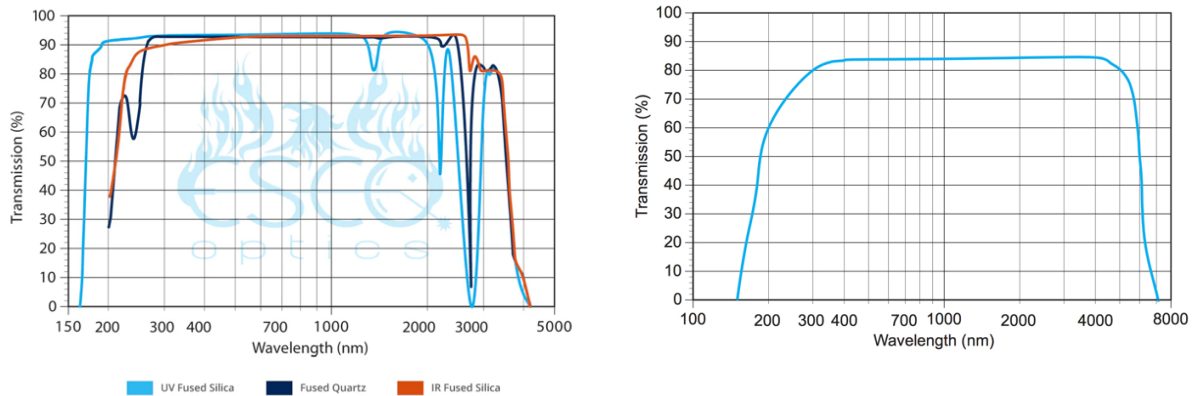


Figure 1a and 1b: Reported transmission for fused silica and sapphire glass from Esco Optics [9][10]

In Elkowitz et al, OES is utilized for dual-mode scramjet control. Part of the control algorithm involved calculating the fuel-to-air equivalence ratio through OES in the scramjet combustor. In this study, a change in optical transmission was observed during the testing period – this change in transmission impacted the calculated equivalence ratio by up to ten percent [8]. The change also impacted the reliability of the control algorithms tested, and after testing a white haze was seen on the windows. This haze was hypothesized to be associated with a change in optical transmission across the entire wavelength range of interest for the facility diagnostics, with an example of impacted UVASCF windows in Figure 2. For PIV and PLIF measurements, the haze led to a poor signal-to-noise ratio, sometimes to the point of precluding useful measurements. The haze therefore affected key wavelengths thus was a significant problem within the UVASCF for obtaining accurate optical and laser-based diagnostic data.

The degradation of the windows is not a new observation. It has existed within the facility for some time, but the cause of the window degradation has not been explored until this point. It had been previously found that the white haze could not simply be cleaned off with cleaning solvents and could only be removed through grinding of the glass surface, leading the investigation into the issue towards some sort of chemical change. After an extensive literature review, a documented process [11-16] in fused silica, devitrification, was identified as the potential process the windows were undergoing.

Devitrification is generally defined as when an amorphous substance, like glass, is held at a sufficiently high temperature for a sufficiently long amount of time and changes into a crystalline phase. Amorphous substances lack long-range order in their molecular structure – the molecules are arranged more like a liquid rather than in an organized form like a solid crystalline structure [11]. In fused silica this change is from the amorphous form of silicon oxide (SiO_2) to its

crystalline form, cristobalite. In fused silica and fused quartz this presents as a milky white haze on or in the glass.

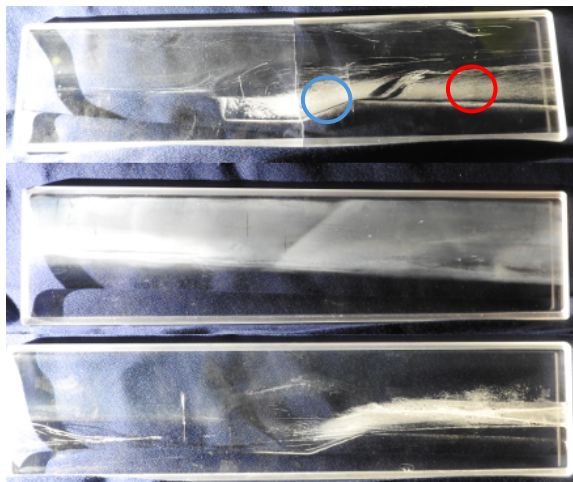


Figure 2: Three example windows, all three windows have been retired from use in testing. The window at the top of the photo is the window used in this study – the crack running across the width of the window occurred after all transmission and x-ray diffraction data was acquired. For transmission testing, location one is in red, location two is in blue.

Studies on devitrification go back over a century, with a study in 1919 linking the temperature glass is held at to crystal formation [12]. Moving forward to 1925, crystallization on laboratory quartzware was studied based on evaporating distilled water from the surface of the glass [13]. It was then found that both persistent heating and cooling cycles as well as the evaporation of water from the surface was the glass was contributing towards crystal formation. In more modern literature, it was known that there are a number of factors that contribute towards devitrification. Water and oxygen were key factors, as the formation of silicon oxide requires an excess of oxygen. Excessively high temperatures and persistent heating and cooling cycles are also a factor. Additionally, it was found that even the highest purity fused silica would eventually devitrify if held about 1,373K (1,100°C) for sufficiently long periods of time, found to be approximately ten hours [14]. Finally, in a 2019 study it was found that NaCl present on the surface of a fused silica window accelerated crystal growth at lower temperatures than expected [15]. Horii et al also states “The devitrification characteristics depend strongly on the temperature, the holding time, silica glass impurities, and contaminants from ambient materials” [15] which agrees with all of the previous literature. Finally, this study looked into if changing the composition of silica glass, in this case to include chlorine, would inhibit devitrification. Modern glassblowing resources agree with all of the above academic literature, specifically citing excess oxygen as a requirement for devitrification to occur along with excessive temperatures and contaminants, implying this process would not occur if experiments were performed in a vacuum [16].

Considering all of the factors that go into the formation of cristobalite in silica glass – temperatures in excess of 1,373 K (1,100°C), long holding times, persistent heating and cooling cycles, and contaminants present on the surface of the glass, the UVASCF is a perfect environment for inducing devitrification in glass. The facility runs for five to six hours at a time, at temperatures in excess of 1,373 K, can expose windows to high temperature water vapor (due to the product of hydrogen and hydrocarbon combustion), and additionally involves liquid fuel injection that may be present on the windows, as well as other possible contaminants from other aspects of the facility operation. The windows can also experience condensation on the windows from the air during startup. Given this information, it was hypothesized the white haze on the windows was indeed cristobalite and the windows are undergoing devitrification while the facility is running. It is therefore the goal of this study to decisively confirm why the transmission of the windows is changing and propose potential solutions.

To support this goal, this study had three main objectives. First, this study seeks to define the problem with the windows in the UVASCF, in this case the windows are experiencing a change in transmission at key wavelengths for optical diagnostics. Second, this study seeks to identify the issue and its potential causes using experimental tools such as x-ray diffraction. This study also seeks to qualitatively assess the amount of damage done to the windows. Third, this study seeks to propose possible solutions for the UVASCF, and other similar facilities, where optical diagnostics are applied and sustained high temperatures are encountered.

Devitrification has not been reported in a hypersonic ground testing facility before, despite the long history of documented devitrification in other fields. This may be because some ground test facilities do not have sufficiently long test durations to see devitrification, or other facilities may be replacing their windows as soon as they show signs of degradation. Nevertheless, this study aims to provide answers for existing facilities and a basis for future facility designers to be aware of when designing new facilities, as well as increase the accuracy of optical diagnostics through retaining transmissivity of the fused silica windows. Potential impacts of this study include changes to how personnel operating high temperature facilities choose window materials and window architectures in order to increase the utility and lifespan of their windows. Additionally, this study seeks to inform decisions about window choice in hypersonic flight vehicles (particularly reusable ones) that may employ optical sensors in the future.

The rest of this paper presents the experimental methodology employed in the study to quantify changes in window optical transmission and the level of cristobalite formation. The results of the experimental methodology for both a used facility windows and virgin samples subjected to a controlled high temperature environment are then presented. Finally, potential solutions are proposed, as well as next steps for study.

2. Experimental Methodology

2.1. Overall Experimental Approach

In the UVASCF there are two larger windows – 0.22m long, 0.05m wide, and 0.01m thick that are located directly on either side of typical flameholding section. The portion in contact with the flameholding area is 0.21m long, 0.04m wide, and 0.01m thick. There is a third, smaller window that is not in close proximity to the flame and will not be discussed in this study. The facility run time is unlimited but often runs in five-hour cycles – two hours to heat up, two hours of testing where combustion occurs, and one hour to cool down.

Addressing the first objective, this experiment was to first look at an existing impacted window to determine the issue. The most appropriate method for identifying the white haze was x-ray diffraction, which would allow for determining what the white haze was, and also if it was crystalline or amorphous. After the phenomenon was successfully identified on an existing window, the next step was to attempt to recreate the white haze in a controlled environment to isolate sustained exposure to high temperatures as a driving factor of the devitrification process.

2.2. Measurements on Existing Facility Windows

Transmission and x-ray diffraction measurements were first applied to a used facility window.

2.2.1. Transmission and X-Ray Diffraction

In Elkowitz et al, a change in transmission of facility windows used during OES testing was identified [8]. This measurement used a spectrometer and white light source to obtain a measure of light transmitted through affected window. The measurements of Elkowitz et al were recreated in this study with a similar with experimental setup, as seen in Figure 3.

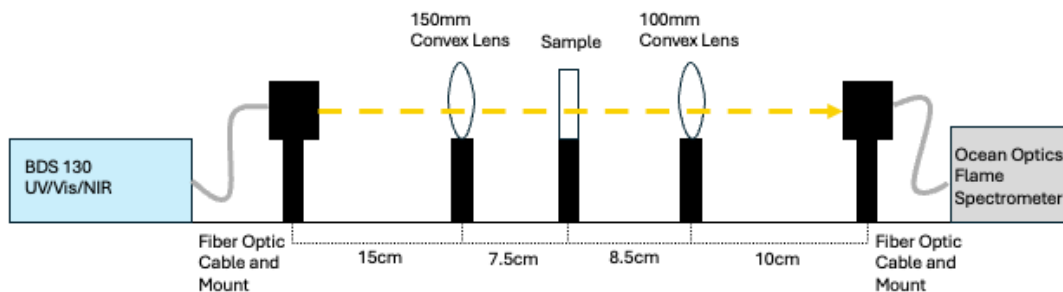


Figure 3: Experimental transmission setup (not to scale) Spectrometer was connected to a computer via USB.

As can be seen in the figure, first the light was routed out of a BDS130 UV/Vis/NIR white light source using an optical fiber. This light was collimated using a 150mm convex lens and passed back through a 100mm convex lens and focused onto the optical fiber routed to the Ocean Optics Flame Spectrometer. A circular area an inch in diameter was measured for consistency

with future testing. The spectrometer was connected to a computer running Ocean View software for data collection.

Three sets of data were taken during transmission measurements with the spectrometer. The spectrometer measured counts of light across the visible spectrum of light. First, the background light or “darks” were taken. Second, the white light source alone was obtained. Finally, the white light source through the window was obtained. To process this data, all scans were averaged together to eliminate small fluctuations between scans. The averaged background light was then subtracted out of the averaged white light source scan and averaged window scan. To derive the transmission of light, the light through the window was divided by the white light alone. This method was used to produce all transmission data in this experiment.

To identify crystalline structures within an amorphous structure such as glass, x-ray diffraction (XRD) is a suitable candidate. X-ray diffraction is possible due to Bragg’s law seen in equation 1.

$$n\lambda = 2d\sin\theta \quad (1)$$

Where n is a whole integer (1, 2, 3...), λ is the wavelength of the incident beam of light, d is the distance between particles in this case, and θ is the half scattering angle. This gives different materials a “fingerprint”, where there is an expected intensity of collected light based on the half scattering angle. Figure 4a and 4b show an image of a window during XRD measurements in a Malvern-Panalytical Empyrean X-Ray Diffractometer and a simplified XRD set-up respectively [17]. X-rays penetrate just below the surface of the sample within a range of 20-100 micrometers.

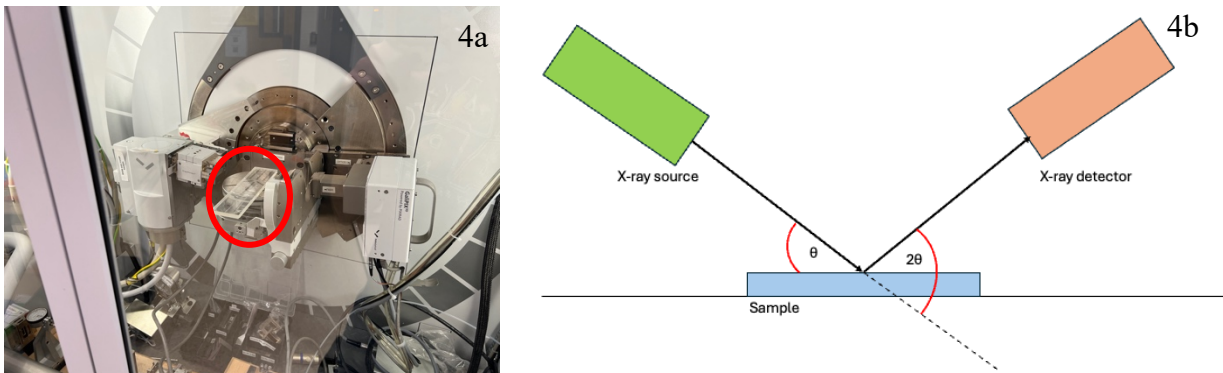


Figure 4a and 4b: Image of the Malvern-Panalytical Empyrean x-ray diffractometer in use (window circled in red) and simplified example of a x-ray diffraction setup for clarity.

X-ray diffraction for the used window was performed in a Malvern-Panalytical Empyrean X-Ray Diffractometer with a Bragg-Bretano HD incident beam PreFIX module. These measurements did not measure the entire window, but rather a small portion in the center of approximately a 0.05m by 0.05m square centered on the most visibly affected area of the window in the flameholding region. This tested area aligns with “Location two” in figure 3.

Processing of the x-ray diffraction data was performed in the open-source software, Profex, using Rietveld Refinement to calculate the relative percentages of material present in the sample [18]. Reference data packaged with Profex was used along with reference data from the Crystallography Open Database [19], [20], [21], [22], [23], [24], [25], [26], [27]. Matching criteria was set to only include material made of silicon oxide.

As mentioned previously, Profex employs the Rietveld refinement method for x-ray diffractometry analysis. The Rietveld refinement method was first introduced for powder x-ray diffractometry in 1969 by H.M. Rietveld. This method was developed to provide more useful numerical data during x-ray diffraction analysis by matching the peak location and relative intensity between observed x-ray diffraction data and standard reference data [28]. The refinement uses the least-squares method to fit a function to the observed diffraction pattern and is iterated automatically until a best-fit is reached. After the function fitting the data is calculated, intensity and peak position between the newly calculated fit and potential phases is compared.

The general process for the Rietveld refinement is as follows:

- 1) Take a known material structure model
- 2) Calculate a theoretical diffraction pattern
- 3) Compare with measured (experimental) data
- 4) Minimize difference between calculated and observed data, and repeat

The model ceases to iterate when $\chi^2 < 1.5$. This method is discussed more in depth below. Differences between the calculated pattern and the observed pattern are minimized by the least-squares method [29].

Three samples of glass were tested along with the existing facility window: a clean sample of UV fused silica, a sample of UV fused silica with a commercial solution meant to prevent devitrification applied, and a sample of sapphire glass. Three matching phases were identified. These phases were silica in its amorphous state, cristobalite (low), and cristobalite (high). Low-cristobalite is metastable at 543K while high-cristobalite is formed at higher temperatures and is stable at 1,743K. Low-cristobalite can transform into high-cristobalite at any temperature in-between 543K to 1,743K [30]. In this case, both forms of cristobalite are present. Profex then ran the refinement, matching the three identified phases to the experimental XRD data. The weight percent of each identified phase of samples is then calculated using known atomic constants [18]. This calculation is only possible due to the accurate matching of phases to observed data via the Rietveld refinement. Detection limits for x-ray diffraction are typically estimated to be about a tenth of a percent. Figure 5 shows an example of reference XRD data used in the refinement process.

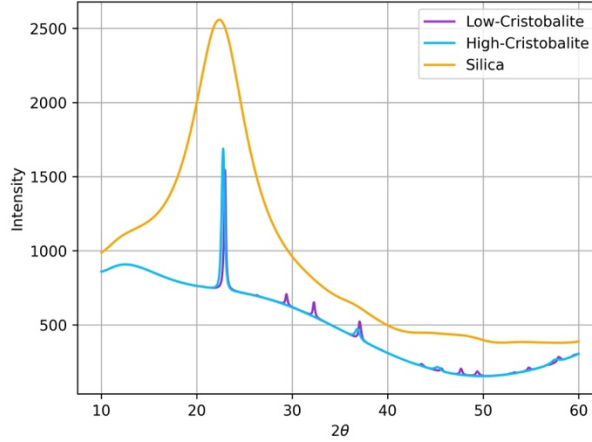


Figure 5: Reference XRD data used in Rietveld refinement

Agreement between the identified peaks and identified data was calculated with the chi-squared test in equation 2, where $O_{2\theta}$ is the observed value and $E_{2\theta}$ is the expected value for every value across 2θ . The closer chi-squared is to one, the better agreement there is between the observed data and the expected data [18], [31].

$$\chi^2 = \sum_{2\theta} \frac{(O_{2\theta} - E_{2\theta})^2}{E_{2\theta}} \quad (2)$$

Profex automatically calculates this value for Rietveld refinement processes and considers any chi-squared value less than 1.5 to be acceptable agreement.

For the samples tested in a controlled environment, all of these steps for both optical transmission and x-ray diffraction remained the same with the exception of the x-ray diffractometer used. The samples subject to the controlled environment were examined in a Rigaku SmartLab X-Ray Diffractometer with Bragg-Bretano optics installed. In this case, the entire surface of the sample is scanned due to its smaller size, and alignment was achieved with calibration of the machine and verified with an alignment camera.

2.3. Transmission of Samples in a Controlled Environment

2.3.1. Summary of Samples Used

The same methods used for the used facility window were employed for the samples used in the controlled environment tests. Three samples in total were tested. First, a clean sample of UV fused silica was testing. This sample was the same thickness as the UVASCF windows. Second, a sample of UV fused silica with a commercial solution for preventing devitrification, Clear Coat Overglaze from Fusion Headquarters Inc., was tested. Third, a sample of sapphire glass from Esco Optics was tested. These samples were tested in a controlled environment and analyzed experimentally before and after the controlled environment tests.

2.3.2. Summary of Controlled Environment

The samples listed above were tested in a Keith 3100 furnace. All samples were cleaned with isopropyl alcohol and handled with gloves prior to going into the furnace to reduce outside contaminants like oil from hands impacting crystal formation, and all samples were laid flat on two ceramic pieces to ensure even heating. The furnace was rated for a maximum safe operating temperature of 1,473 K (1,200°C). A ten-hour cycle was programmed into the furnace to mimic the length of testing time the UVASCF windows were exposed to. Additionally, it takes longer for the furnace to cool down than the combustion facility, so a two-hour portion of time is dedicated to tracking the cooldown process. The program first ramps up to 1,203K (930°C) and held there for an hour. This is the stagnation temperature of the UVASCF. The furnace then ramped up to 1,473K, the maximum safe temperature for the furnace. This maximum temperature was used to simulate hotter areas of the facility, to approximate flameholding areas, and is held at this temperature for roughly two hours.

The furnace temperatures were measured every hour with a Type-K thermocouple and compared against air temperature in a typical UVASCF run, as seen in Figure 6. The Type-K thermocouple measurement has an estimated uncertainty of $\pm 0.42\text{K}$ (0.42°C) [32]. It is important to note that during UVASCF testing, the temperature in the flameholding region is significantly higher than the plotted stagnation temperature of Figure 6 due to the presence of combustion, but the window temperature would not exceed 2,000K, as that is the maximum measured temperature in the flameholding region.

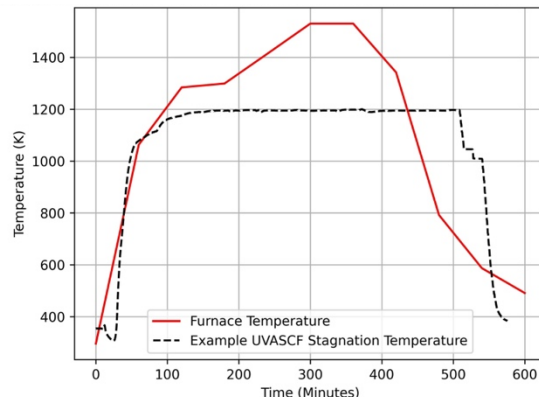


Figure 6: Temperature data from the furnace vs. stagnation temperature during a UVASCF test

The controlled environment of the furnace was chosen to isolate heat as one of the key factors of devitrification. As discussed earlier, devitrification can be accelerated by many factors, but as stated in Brockner et al devitrification will occur if glass is held at a high temperature in excess of 10 hours, even if the glass is extremely high purity [14]. This controlled environment test does not account for contaminants in the air flow of the facility, such as water vapor or fuel, and only simulates one heating and cooling cycle of the UVASCF. Therefore, less devitrification may be expected.

3. Results

The results for this study are presented as follows. First, the results for the existing used facility window will be discussed, including optical transmission and x-ray diffraction. Second, the results for the virgin samples tested in the controlled environment will be discussed, for both before and after exposure to high temperature of the controlled environment.

3.1. Existing Facility Windows

3.1.1. Transmission

Transmission through the used facility window shows dramatic deviation from a virgin sample. The window measured is the uppermost window seen in Figure 2. Figure 7 shows a loss in transmission of over 50% at around 400nm at both locations one and two, with transmission at any given wavelength never exceeding 60%.

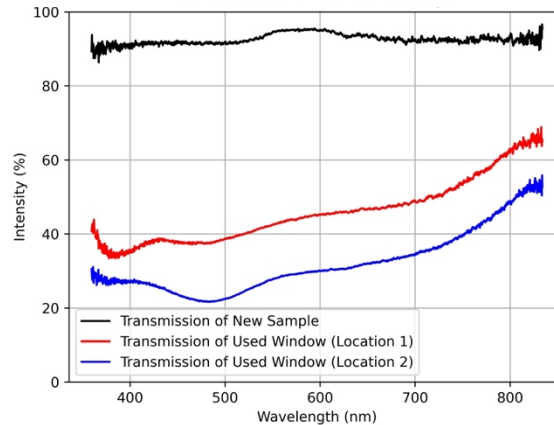


Figure 7: Measured transmission of used window at two different versus new sample from Esco Optics.

The impact on OES measurements is immediately obvious as the transmission across the entire visible wavelength spectrum has degraded significantly. As for other diagnostics discussed in the text – at 527nm and 532nm transmission drops below 30% at location 2, which severely impacts the ability of a Nd:YLF or Nd:YAG laser beam to enter the flowpath, leading to a deterioration in the signal-to-noise ratio for PIV. CARS measurements rely on 400nm, 532nm, 674nm, or 800nm depending on the type of CARS being implemented and the measurements taken, but every wavelength except for 800nm never has a higher transmission than 50%, once again leading to a deterioration of SNR during testing. This window was determined by facility staff to be unusable, and this set of transmission data demonstrates why this decision was made.

The number of times each window was used in a UVASCF run was not tracked, but the windows are typically reused until their transmission becomes insufficient for testing before being retired. This measurement is therefore representative of the state of transmission at the end of the lifetime of the facility windows.

3.1.2. X-Ray Diffraction

Figure 8 shows the x-ray diffraction measurements for a used facility window alongside different phases of cristobalite and silica for reference. In Figure 8, “Observed XRD Data” refers to the initial XRD dataset measured. “Fitted Data” is the fitted curve calculated by the Rietveld refinement and “Difference” is the difference between the XRD data and the Rietveld refinement. “Low-Cristobalite” is low-cristobalite, “High-Cristobalite” is high-cristobalite, and “Silica” is silica in its amorphous state. “Background” is background x-ray radiation as determined by the specific diffractometer used. This naming scheme is the same for all x-ray diffraction data in this paper.

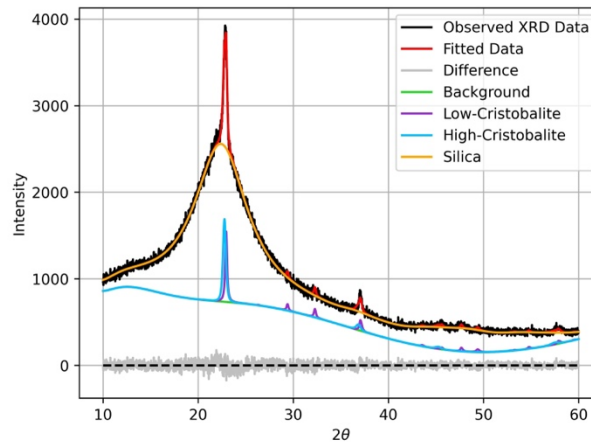


Figure 8: X-ray diffraction data for used facility window

It can be seen in the figure that there is a broad peak from a 2θ of 17 degrees to a 2θ of 30, which is indicative of an amorphous substance. Narrow peaks are indicative of a crystalline structure. There is a narrow peak at $2\theta = 22$ in the middle of the amorphous structure. This indicates a crystalline structure within an amorphous structure. The main peak at the half-scattering angle of 22 degrees aligns with the mean peak documented in cristobalite samples from the databases. There are two smaller peaks at 31 and 36 degrees that also agree with the existing diffraction data for cristobalite. A Rietveld refinement was performed to calculate both agreement between the identified peaks, the identified material candidates (cristobalite), and if agreement between half-scattering angle location and relative intensity was sufficient, the relative quantity of the structure was also calculated.

Table 1 shows the calculated data from the Rietveld refinement for all three refinements done in this study, as well as the chi-squared metric for each case. This is the calculated relative percentage of the sample at different phases. Only phases containing silicon and oxygen were considered for clarity in processing and the reported chi-squared value was 1.1944. The closer the chi-squared value is to one, the better agreement there is between the fitted refinement data, and the XRD data. In this case, a chi-squared of 1.1944 is regarded as good agreement. The reported standard deviation is calculated from the difference between the initial XRD scan and the refinement [33]. The standard deviation is then multiplied by a factor of 2.77 to calculate the

Least Significant Change (LSC) which is consistent with a 95% confidence interval [34]. This encompasses all error, both random and systematic.

Low-cristobalite and high-cristobalite refer to crystalline structures present and silica is an amorphous structure. In this used window, $95.75 \pm 0.748\%$ of the window has remained in an amorphous “glassy” state. Across both different crystalline states, $4.21 \pm 0.770\%$ of the window’s total measured volume has become crystalline with a reasonable experimental uncertainty that does not negate the calculated amounts of the substances.

Table 1: Weight percents of the samples calculated by Rietveld refinement

	Used Facility Window	Sample, Pre-Furnace	Sample, Post-Furnace
Low-Cristobalite	2.41±0.471%	0±0%	0.221±0.211%
High-Cristobalite	1.8±0.609%	0.113±0.263%	0.243±0.230%
Silica	95.75±0.748%	99.89±0.263%	99.54±0.332%
Chi-Squared	1.1944	1.1550	0.9420

3.2. Controlled Environment Samples

Once cristobalite was identified within existing facility windows, smaller samples of virgin glass were obtained. This included UV-fused silica and sapphire glass. These controlled samples were then subject to a 10-hour cycle in the furnace in order to mimic a testing cycle in the facility. Optical transmission and x-ray diffraction data was then taken both before and after this cycle and compared. After the fused silica sample went through the 10-hour furnace cycle, there was a white speckling visible on the surface of the sample.

3.2.1. Transmission

The fused silica sample showed clear losses after the controlled cycle in the furnace. As shown in Figure 9, there is a consistent loss of between 5 and 10% in the 400-800nm range, with some wavelengths affected notably worse than others. There is consistent loss in transmission across the entire measured spectrum, with an approximate 8% loss in transmission across the range.

There are notable differences from the transmission tests done on the used window but considering the inconsistent way devitrification forms on the windows due to combustion, and the difference in window exposure duration, this is a possibility. The transmission losses across the used facility window are much greater, with some wavelengths only transmitting 20% of the light.

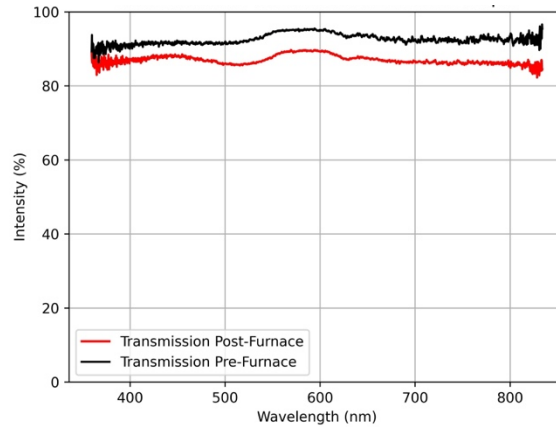


Figure 9: Change in transmission after heat cycle for controlled sample

This controlled environment test is only meant to mimic one heating and cooling cycle in the UVASCF. Despite only being a simulation of one testing cycle, there is a notable loss in transmission at nearly every measured wavelength. The measured loss in transmission successfully isolates heat as a main factor in window degradation.

3.2.2. X-Ray Diffraction

X-ray diffraction data was processed for the fused silica samples in Profex. Two sets of x-ray diffraction data were taken – one before the heat treatment in the furnace and one afterwards. The same material candidates identified and used for the UVASCF facility window were used for the Rietveld refinement of the samples.

Figure 10 is the graph of the x-ray diffraction data from before heat treatment. Unlike the UVASCF window there are no narrow peaks around $2\theta = 22$, just one broad amorphous peak from $2\theta = 17$ to $2\theta 30$. There is no agreement between the cristobalite diffraction patterns, and the sample tested.

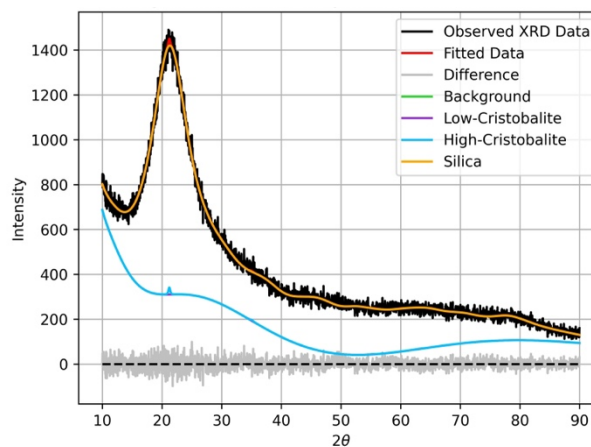


Figure 10: X-ray diffraction data for sample before heat treatment

Table 1 shows the calculated results for the sample before heat treatment. The reported chi-squared indicated a good fit between the fitted data and the actual data taken as discussed earlier in the text.

There is a negligible amount of crystallization in the sample before the controlled environment testing. It is determined that $99.89 \pm 0.263\%$ of the sample is still in an amorphous silica form. No cristobalite was detected in the sample before the heat treatment. There is no low-cristobalite detected at all, and the 0% uncertainty reflects no calculated weight percent due to no match identified between the Rietveld refinement and the data taken.

This sample was then subject to a 10-hour testing window in the furnace as shown in Figure 5. Figure 11 is the graph of the x-ray diffraction data alongside reference data. The report chi-squared also indicated an extremely good agreement in this fit.

This x-ray diffraction data is not as dramatic as the x-ray diffraction for the facility window, however there are notable changes in the pattern when compared to Figure 10. There is a small peak at $2\theta = 22$ in both the observed and the fitted curve. Similarly to the facility windows, and in alignment with the cristobalite reference data. There also appears to be a smaller peak at $2\theta = 36$. These peaks are not present in Figure 10, x-ray diffraction of the same sample before heat treatment, but are present in Figure 8, the x-ray diffraction of a used facility window.

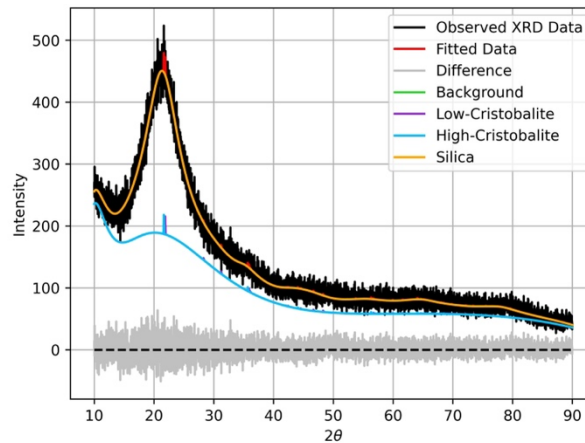


Figure 11: X-ray diffraction data for sample after heat treatment

The lower intensity of these peaks implies less of the crystalline substance within the glass. This is consistent with the testing done – the furnace cycle is meant to isolate high temperature as a contributing factor and additionally only simulate the UVASCF running once.

Table 1 also shows the Rietveld refinement data for the post-furnace sample, which agrees with this conclusion. The sample after heat treatment in the furnace is estimated at 0.464% of the measured sample as either low-cristobalite or high-cristobalite, while the untreated sample is estimated at 0.133% high cristobalite, with an error that could make this value zero. For reference, the used window is estimated to be 4.21% cristobalite.

Compared to the used UVASCF window there is significantly less cristobalite present. However, this sample was only put through one high temperature test with no other contaminants. The UVASCF window went through between two and fifteen tests in the facility and was exposed to high temperatures and contaminants.

These calculations estimate $0.464 \pm 0.312\%$ of the sample has become crystalline. This change is significant when coupled with the loss of transmission of this sample – a piece of virgin fused silica had loss in transmission across the measured range and had a measurably different structural makeup after prolonged exposure to high temperature and thus isolating the primary factor in window degradation.

3.3. Sapphire Samples

A sample of sapphire glass sourced from Esco Optics was also exposed to the same 10-hour cycle in the furnace as the UV-fused silica sample. The sample of sapphire glass did not show any loss of transmission after a cycle in the furnace. This was expected, as sapphire is already in a crystalline state and by definition cannot devitrify and is well-documented to survive high temperatures.

4. Discussion

In this study it was found through x-ray diffraction that existing facility windows with degraded transmission exhibited diffraction patterns consistent with cristobalite. This finding clearly indicates that fused silica windows in the UVASCF are devitrifying during the testing time for the facility, and the loss in optical transmission is the result of devitrification. This finding answered the question posed in Elkowitz et al as to why the OES control scheme ultimately was unable to accurately calculate the equivalence ratio. Due to the presence of high-cristobalite in the existing facility window, it can now be estimated the window surface temperature was between 1,743K-2,000K, the stable temperature of high-cristobalite and the measured maximum temperature in the flameholding region.

Second, high temperature was isolated as a main factor in the devitrification process through the controlled environment tests. A sample of virgin fused silica glass both exhibited devitrification and a notable loss in transmission after ten hours in the controlled furnace environment, reaching a maximum temperature in excess of 1,473K (1,200°C). The sample tested in the controlled environment was 3.4 times less devitrified by volume than the existing UVASCF window. This was an expected outcome, as the sample experienced a simulation of a single run time.

Additionally, it was found that sapphire glass did not devitrify in the furnace. A commercial ceramics solution was also tested, but this solution failed due to exposure to higher temperatures than the glaze was rated for.

The first proposed solution for the UVASCF and other similar facilities is to use sapphire windows where possible. Figure 1b demonstrates the transmission characteristics of sapphire glass, showing transmission suffering below 400nm. Due to the lack of transmission at lower wavelengths, this solution is not always viable, specifically for PLIF or CARS diagnostics that require transmission around 200nm. Sapphire glass is roughly three times as expensive as fused silica glass. Thus, for the use of sapphire glass in the UVASCF to be a cost-effective solution, each must survive longer than three fused silica windows. This solution is likely best served for small windows, and windows on reusable flight vehicles due to the higher cost of sapphire.

Environmental barrier coatings can also be used to stop devitrification by preventing oxygen from reacting with a glass, a key component of the devitrification process. The work in Xiao et al focuses on ceramic matrix composites to improve silicon oxide survivability in combustion engines and combustion environments [35]. Similarly, the work in Chen et al also focuses on ceramic matrix composites for combustion environments like Xiao et al, specifically suggesting yttrium, ytterbium, and lutetium silicates [35], [36]. Both studies are focused on preventing corrosion of silicates and do not test for optical transmissivity. Other environmental barrier coating suggestions come in the form of different coatings or depositing techniques. In Bolelli et al plasma sputtering was tested for the purpose of depositing environmental barrier coatings onto silicates and showed it does prevent devitrification, however, also concludes that the method is not ready for large scale production [37]. The work in Minami et al is the only option discussed here that touches on optical transmissivity for the studied coating – an aluminum doped zinc oxide film. This film lacks transmissivity below 300nm and was not tested at temperatures as hot as the UVASCF achieves but could potentially be tested in the future [38]. Identifying an environmental barrier coating for the exact purposes of the UVASCF and other facilities is possible, but would likely require further research, as no coating has been developed for this exact purpose yet.

Film cooling is also a potential solution. This entails a separate, cooler air stream being blown over the surface of the window facing the flame. Specific geometry configurations will vary from facility to facility, but Cary et al found film cooling in hypersonic environments to be more effective than film cooling in slower environments [39]. However, it was also found in highly turbulent environments, film cooling suffers in effectiveness [40]. Ultimately, the implementation of film cooling will be configuration dependent as film cooling performance is affected by a number of factors, including but not limited to shape of the cooling hole, injection angle of the cooling hole, and mass flux ratio [41]. Additionally, it was found at high mass flux ratios, the cooling stream may detach from the wall, which would negate the benefits of film cooling altogether [42]. Finally, optical diagnostics applications in the facility should be take into account the turbulent mixing layer and density gradient introduced as they can also interfere with optical diagnostics.

There are also alternative silica compositions that present an interesting option. The optical transmission of these materials is not as widely tested or reported but are worthwhile to consider

testing for hypersonic ground facilities. Jau-Ho et al tests for a critical value of alumina within borosilicate glass. While borosilicate glass is not suitable for the high temperatures of the UVASCF, it was found that alumina within the glass reacted with sodium and created a protective layer faster than cristobalite could be produced [43]. Horii et al also found that chlorine doped silica was resistant to devitrification as well [15].

This study would benefit in further characterizing the rate of crystal formation in fused silica. Specifically, studying x-ray diffraction patterns as both a function of temperature and time to track how crystals form as the temperature increases. This type of measurement is possible in x-ray diffractometers with “hot stages” that increase temperature over time in the machine. For further controlled environment testing, a sample should be cycled in a furnace more than once. Additionally, the transmission can be tested in real time as the facility operates and x-ray diffraction can be done after each test cycle. Additionally, to get a more accurate quantification, future x-ray diffraction data should be taken with the goal of reducing noise in the reading. Another consideration is that due to the entire sample being heated evenly, there may be cristobalite present within the sample deeper than the x-ray can penetrate, leading to the possibility that there is crystalline material unaccounted for.

5. Conclusion

The results of this study show that the windows in the UVASCF are undergoing devitrification over the testing time in the facility, turning the amorphous fused silica into crystalline cristobalite. This change creates a milky white appearance on the glass and reduces transmission of the visible wavelength spectrum. Through controlled environment testing, high temperature was identified as a key cause of this phenomenon, as a sample of virgin glass also devitrified in a test that mimicked the high temperatures and long test times of the facility.

Devitrification of optical windows has not been previously reported in a hypersonic ground testing facility. Identification of this phenomenon and its key cause will inform operators of other facilities on ways to potentially avoid the detrimental effects in their own facility. In the future, different compositions of glass should be considered for use. Operators of similar facilities should be aware of this issue during planning stages and should design around it accordingly, either by pursuing alternate glass materials, replacing fused silica windows more often, or reducing run times.

Additionally, the results of this study inform designers of future reusable flight vehicles of a potential problem with windows for optical sensors. In reusable flight vehicles, alternate crystalline glasses such as sapphire is a necessity for longevity, as sapphire glass cannot devitrify at all. By identifying the problem and isolating the cause, both the hypersonic ground and flight test communities are better positioned to explore potential solutions.

Appendix A – Sapphire Transmission Data

The sapphire sample did not show any meaningful losses in transmission, as seen in Figure A.

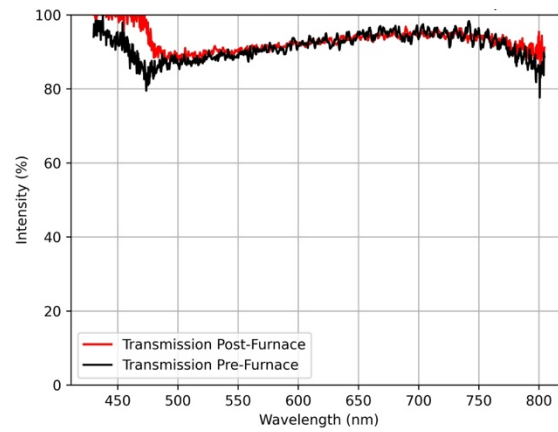


Figure A: Sapphire sample transmission before and after heat treatment

Bibliography

- [1] J. Anderson, “Hypersonic Flow-What Is It?,” in *Hypersonic and High Temperature Gas Dynamics*, 2nd ed., Reston, VA: American Institute of Aeronautics and Astronautics, 2000, ch. 1, pp. 13–23.
- [2] M. Smart, “Scramjets,” *The Aeronautical Journal*, vol. 111, no. 1124, pp. 605–619, 2007, doi: 10.1017/S0001924000004796.
- [3] National Aeronautics and Space Administration, “NASA’S X-43A Scramjet Breaks Speed Record.” Accessed: Mar. 05, 2025. [Online]. Available: <https://www.nasa.gov/news-release/nasas-x-43a-scramjet-breaks-speed-record/>
- [4] United States Air Force, “X-51 Waverider makes historic hypersonic flight.” Accessed: Mar. 05, 2025. [Online]. Available: <https://www.af.mil/News/Article-Display/Article/116538/x-51-waverider-makes-historic-hypersonic-flight/>
- [5] A. J. Kim, “High-Resolution fs/ps CARS for Quantitative Measurements of Temperature and Species in a Dual-Mode Scramjet,” 2023.
- [6] C. D. Mcrae *et al.*, “OH PLIF Visualization of the UVa Supersonic Combustion Experiment: Configuration C”.
- [7] K. Song *et al.*, “Advances in Femtosecond Coherent Anti-Stokes Raman Scattering for Thermometry,” *Photonics 2024, Vol. 11, Page 622*, vol. 11, no. 7, p. 622, Jun. 2024, doi: 10.3390/PHOTONICS11070622.
- [8] L. Elkowitz, A. Wanchek, R. Rockwell, C. P. Goyne, and C. E. Dedic, “Dual-mode scramjet control using optical emission sensors,” *Appl Opt*, vol. 63, no. 5, p. 1355, Feb. 2024, doi: 10.1364/ao.507587.
- [9] Esco Optics Inc., “Materials Data - Fused Silica / Fused Quartz | Esco Optics – Esco Optics, Inc.” Accessed: Mar. 07, 2025. [Online]. Available: <https://escooptics.com/pages/materials-fused-silica-quartz>
- [10] Esco Optics Inc., “Sapphire-Grade | Material Data | Esco Optics, Inc.” Accessed: Mar. 07, 2025. [Online]. Available: <https://escooptics.com/pages/sapphire>
- [11] Z. Q. Hu, A. M. Wang, and H. F. Zhang, “Amorphous Materials,” *Modern Inorganic Synthetic Chemistry: Second Edition*, pp. 641–667, Jan. 2017, doi: 10.1016/B978-0-444-63591-4.00022-7.
- [12] N. L. Bowen, “DEVITRIFICATION OF GLASS,” *Journal of the American Ceramic Society*, vol. 2, no. 4, pp. 261–281, Apr. 1919, doi: 10.1111/J.1151-2916.1919.TB17505.X.

- [13] F. C. Vilbrandt, "Elimination of Surface Devitrification on Laboratory Quartzware," *Ind Eng Chem*, vol. 17, no. 8, pp. 835–837, Aug. 1925, doi: 10.1021/IE50188A026/ASSET/IE50188A026.FP.PNG_V03.
- [14] R. Brockner, "PROPERTIES AND STRUCTURE OF VITREOUS SILICA," 1970.
- [15] N. Horii, A. Inouye, N. Kuzuu, and H. Horikoshi, "Effect of suppression of devitrification by chlorine-containing silica glass," *Journal of the Ceramic Society of Japan*, vol. 127, no. 10, pp. 773–776, 2019, doi: 10.2109/jcersj2.19108.
- [16] Precision Glassblowing, "Devitrification and Solarization." Accessed: Mar. 05, 2025. [Online]. Available: <https://precisionglassblowing.com/devitrification-and-solarization/>
- [17] D. Henry, N. Eby, J. Goodge, and M. David, "X-ray reflection in accordance with Bragg's Law." Accessed: Mar. 08, 2025. [Online]. Available: https://serc.carleton.edu/msu_nanotech/methods/BraggsLaw.html
- [18] N. Doebelin and R. Kleeberg, "Profex: a graphical user interface for the Rietveld refinement program BGMN," *urn:issn:1600-5767*, vol. 48, no. 5, pp. 1573–1580, Aug. 2015, doi: 10.1107/S1600576715014685.
- [19] R. T. Downs and M. Hall-Wallace, "The American Mineralogist crystal structure database," *American Mineralogist*, vol. 88, no. 1, pp. 247–250, 2003.
- [20] A. Vaitkus *et al.*, "A workflow for deriving chemical entities from crystallographic data and its application to the Crystallography Open Database," *J Cheminform*, vol. 15, no. 1, pp. 1–15, Dec. 2023, doi: 10.1186/S13321-023-00780-2/FIGURES/5.
- [21] A. Merkys, A. Vaitkus, A. Grybauskas, A. Konovalovas, M. Quirós, and S. Gražulis, "Graph isomorphism-based algorithm for cross-checking chemical and crystallographic descriptions," *J Cheminform*, vol. 15, no. 1, pp. 1–13, Dec. 2023, doi: 10.1186/S13321-023-00692-1/TABLES/1.
- [22] A. Vaitkus, A. Merkys, and S. Gražulis, "Validation of the Crystallography Open Database using the Crystallographic Information Framework," *J Appl Crystallogr*, vol. 54, no. 2, pp. 661–672, Apr. 2021, doi: 10.1107/S1600576720016532/YR5065SUP1.PDF.
- [23] M. Quirós, S. Gražulis, S. Girdzijauskaitė, A. Merkys, and A. Vaitkus, "Using SMILES strings for the description of chemical connectivity in the Crystallography Open Database," *J Cheminform*, vol. 10, no. 1, pp. 1–17, Dec. 2018, doi: 10.1186/S13321-018-0279-6/TABLES/4.
- [24] A. Merkys, A. Vaitkus, J. Butkus, M. Okulič-Kazarinas, V. Kairys, and S. Gražulis, "COD::CIF::Parser: An error-correcting CIF parser for the Perl language," *J Appl Crystallogr*, vol. 49, no. 1, pp. 292–301, Feb. 2016, doi: 10.1107/S1600576715022396/PO5052SUP3.TGZ.

- [25] S. Gražulis, A. Merkys, A. Vaitkus, and M. Okulič-Kazarinas, “Computing stoichiometric molecular composition from crystal structures,” *J Appl Crystallogr*, vol. 48, no. 1, pp. 85–91, Feb. 2015, doi: 10.1107/S1600576714025904/KK5188SUP1.ZIP.
- [26] S. Gražulis *et al.*, “Crystallography Open Database (COD): an open-access collection of crystal structures and platform for world-wide collaboration,” *Nucleic Acids Res*, vol. 40, no. D1, pp. D420–D427, Jan. 2012, doi: 10.1093/NAR/GKR900.
- [27] S. Graulis *et al.*, “Crystallography Open Database – an open-access collection of crystal structures,” *urn:issn:0021-8898*, vol. 42, no. 4, pp. 726–729, May 2009, doi: 10.1107/S0021889809016690.
- [28] H. M. Rietveld, “A profile refinement method for nuclear and magnetic structures,” *urn:issn:0021-8898*, vol. 2, no. 2, pp. 65–71, Jun. 1969, doi: 10.1107/S0021889869006558.
- [29] N. Döebelin, “Lesson 3: Basics of Rietveld Refinement,” <https://www.profex-xrd.org/wp-content/uploads/2024/03/FZJ-03-Rietveld-Refinement-Basics.pdf>.
- [30] The Quartz Page, “Overview of Silica Polymorphs.” Accessed: Mar. 12, 2025. [Online]. Available: http://www.quartzpage.de/gen_mod.html
- [31] A. Biswal, “Chi-Square Test: Formula, Types, & Examples.” Accessed: Mar. 08, 2025. [Online]. Available: <https://www.simplilearn.com/tutorials/statistics-tutorial/chi-square-test>
- [32] Y. Yen Kee, Y. Asako, T. Lit Ken, and N. Azwadi Che Sidik, “Uncertainty of Temperature measured by Thermocouple,” *Journal of Advanced Research in Fluid Mechanics and Thermal Sciences Journal homepage*, vol. 68, pp. 54–62, 2020, doi: 10.37934/arfmts.68.1.5462.
- [33] Jörg Bergmann, *Rietveld Analysis Program BGMN*, 4th ed. Dresden, Germany, 2005.
- [34] ASTM International, “Standard Practice for Use of the Terms Precision and Bias in ASTM Test Methods,” Oct. 01, 2020, *ASTM International, West Conshohocken, PA*. doi: 10.1520/E0177-20.
- [35] S. Xiao *et al.*, “Evaluation of environmental barrier coatings: A review,” *Int J Appl Ceram Technol*, vol. 20, no. 4, pp. 2055–2076, Jul. 2023, doi: 10.1111/IJAC.14370.
- [36] Z. Tian *et al.*, “Corrosion of RE₂Si₂O₇ (RE=Y, Yb, and Lu) environmental barrier coating materials by molten calcium-magnesium-alumino-silicate glass at high temperatures,” *J Eur Ceram Soc*, vol. 39, no. 14, pp. 4245–4254, Nov. 2019, doi: 10.1016/J.JEURCERAMSOC.2019.05.036.

- [37] G. Bolelli, L. Lusvarghi, T. Manfredini, and C. Siligardi, “Devitrification behaviour of plasma-sprayed glass coatings,” *J Eur Ceram Soc*, vol. 27, no. 2–3, pp. 623–628, Jan. 2007, doi: 10.1016/J.JEURCERAMSOC.2006.04.119.
- [38] T. Minami, H. Nanto, and S. Takata, “Highly Conductive and Transparent Aluminum Doped Zinc Oxide Thin Films Prepared by RF Magnetron Sputtering,” *Jpn J Appl Phys*, vol. 23, no. 5, pp. L280–L282, May 1984, doi: 10.1143/JJAP.23.L280/XML.
- [39] A. M. Cary and J. N. Hefner, “Film cooling effectiveness in hypersonic turbulent flow,” <https://doi.org/10.2514/3.6062>, vol. 8, no. 11, pp. 2090–2091, May 2012, doi: 10.2514/3.6062.
- [40] J. P. Bons, C. D. MacArthur, and R. B. Rivir, “The Effect of High Free-Stream Turbulence on Film Cooling Effectiveness,” *J Turbomach*, vol. 118, no. 4, pp. 814–825, Oct. 1996, doi: 10.1115/1.2840939.
- [41] U.S. Department of Energy-National Energy Technology Laboratory (NETL), L. Smith, H. Karim, S. Etemad, and W. C. Pfefferle, *The Gas Turbine Handbook*. Morgantown, WV: National Energy Technology Lab (NETL), 2006.
- [42] A. K. Sinha, D. G. Bogard, and M. E. Crawford, “Film-Cooling Effectiveness Downstream of a Single Row of Holes With Variable Density Ratio,” *J Turbomach*, vol. 113, no. 3, pp. 442–449, Jul. 1991, doi: 10.1115/1.2927894.
- [43] J. -H Jean and T. K. Gupta, “Alumina as a Devitrification Inhibitor during Sintering of Borosilicate Glass Powders,” *Journal of the American Ceramic Society*, vol. 76, no. 8, pp. 2010–2016, Aug. 1993, doi: 10.1111/J.1151-2916.1993.TB08325.X.